

Calculation of the Equivalent Dose of the First and the Most Important Secondary Particles in Brain Proton Therapy by Monte Carlo Simulation

Nasim Alsadat Mousavi ¹, Alireza Karimian ^{2*}, Mohammad Hassan Alamatsaz ¹

1. Department of Physics, Faculty of Physics, Isfahan University of Technology, Isfahan, Iran
2. Department of Biomedical Engineering, Faculty of Engineering, University of Isfahan, Isfahan, Iran

| ARTICLE INFO | ABSTRACT |
|---|---|
| <p>Article type: Original Article</p> <hr/> <p>Article history: Received: Aug 01, 2018 Accepted: Jan 02, 2019</p> <hr/> <p>Keywords: Brain Tumor Monte Carlo Method Proton Therapy</p> | <p>Introduction: Due to nuclear interactions between the tissues and high-energy protons, the particles, including neutrons, positrons, and photons arise during proton therapy. This study aimed at investigating the dose distribution of proton and secondary particles, such as positrons, neutrons, and photons using the Monte Carlo method.</p> <p>Material and Methods: In this study, a beam of protons was utilized with the energies of 160 and 190 MeV, which are more popular for brain tumor treatment. This beam irradiated the brain phantom after passing through proton therapy nozzle components. This phantom has a tumor with a radius of 3 cm in its centre. The most important parts of the nozzle include magnetic wobbler, scatterer, ridge filter, and collimator.</p> <p>Results: The results show that while using protons with the energy values of 190 and 160 MeV, the equivalent dose fractions in tumor, brain, skull, and skin to the total equivalent dose in the head are 61.8 (62.4%), 10.4(10.9%), 6.07(3.69%), and 21.7(23%), respectively, regarding the primary and secondary particles.</p> <p>Conclusion: According to the obtained results, in spite of the fact that most of the equivalent dose was inside the tumor volume, the skin of head has received the noticeable dose during proton therapy of brain which needs more concern.</p> |

► Please cite this article as:

Mousavi N, Karimian A, Alamatsaz M.H. Calculation of the Equivalent Dose of the First and the Most Important Secondary Particles in Brain Proton Therapy by Monte Carlo Simulation. Iran J Med Phys 2019; 16: 341-348. 10.22038/ijmp.2019.32424.1386.

Introduction

Due to fewer side effects and the highest level of efficiency, proton therapy is considered as one of the best treatments of brain cancers which leaves much less damage to healthy tissue. Unfortunately, this technology is very expensive and it is available only in a few medical centres worldwide. In addition, doses delivered to the tissue and tumor need more consideration because of the secondary particles (1-3). Therefore, due to the importance of doses delivered to normal and tumoral tissues, there have been interests to carry out research in this regard. For instance, Farahet et al. (4) investigated the dose of neutron during proton therapy of ocular melanoma tumor and craniopharyngioma (intracranial tumor) using Monte Carlo and MCNPX code. They have utilized two phantoms, namely Medical Internal Radiation Dose (MIRD) and University of Florida Hybrid adult male phantom (UFHADM) for about 20 different organs, including eye, brain, and thyroid. The proton energies in this study were considered as 75 and 178 MeV. Moreover, Zheng et al. (5) in 2007 have conducted some studies on neutron equivalent dose in proton therapy using passive technique, a cylindrical

water phantom, and Monte Carlo method. They calculated the value of (H/D) as a function of effective factors on treatment planning, such as proton energy, location of the patient in the treatment room, visibility, and the width of Bragg peak. Accordingly, H denotes neutron equivalent dose and D signifies the therapeutic absorbed dose. In 2012, Zheng et al. (6) attempted to measure the equivalent dose (H) on the absorbed dose of treatment (D) for neutrons (H/D) in pencil beam scanning proton therapy.

They used a neutron detector to calculate the value of (H/D) at a distance of 50 cm from cylindrical water phantom, as a function of proton range, modulation width, beam scanning area, collimator opening hole, and other effective factors on neutron equivalent dose. These factors include components of diaphragm and presence or absence of the compensator. The results showed that the value of (H/D) increased with the increase of proton range and modulation width. In 2016, Geng et al. (7) assessed the delivered risk to the fetus by scattered neutrons in proton therapy of the brain during pregnancy. They used Monte Carlo

*Corresponding Author: Tel: +98 (031) 37934059; Fax: +98 (031) 37932771; E-mail: karimian@eng.ui.ac.ir

interaction with the target nuclide in energy of E (barn), and $\phi(E)$ signifies the fluence of protons ($\frac{1}{cm^2}$).

If the integral is divided into a very small range of energy, $\delta(E)$ and $\phi(E)$ can be considered as constant numbers; therefore, reaction rate value can be obtained using DE and DF cards in MCNPX code. Figure 2 depicts the cross-section versus the energy of the proton in the production of some positron emitters. The value of δ in equation (1) was calculated using the values of this figure which was adapted from TENDL reports updated in 2014 (11).

Simulation

The Hyogo Ion Beam Medical Centre (HIBMC) (12) was simulated in this study. As shown in Figure 3, this centre uses advanced scattering beam delivery method. Therefore, the output beam from the accelerator (Z direction) must be shaped in lateral and longitudinal directions (X and Y). In advanced scattering method, the beams pass through Magnetic Wobbler and then scatterer in order to flat the beam in the lateral direction. Bragg peak can be flattened by a ridge filter. The flattened proton beam then passes through the collimator. The collimator and range compensator make the beam shape as similar as possible to the geometrical

shape of the tumour. In this structure, the range shifter is responsible for flattening the Bragg peak according to the tumor position inside the patient’s body. The collimator and range compensator make the beam shape as similar as possible to the geometrical shape of the tumour. The monitors control the uniformity of the radiation; however, they do not affect the shape or energy of the beam.

The simulation and calculation of the proper characteristics of the above components of the proton therapy system are explained as follows:

The output beam of the accelerator has a very small diameter. To use this beam, it must be expanded by a Wobbler magnet. Its path is followed by Eq.2. Moreover, the used conditions by Riazi et al. (13) were assumed considering the magnetic field. The beam of a proton with the energy of 190 MeV was affected by the magnetic fields of 0.18 and 0.21 T in x and y directions, respectively, in a sinusoidal pattern with a frequency of 60 Hz. Such a beam then takes the form of a cone with the vertex angle of 1.94 degrees (Figure 4).

$$\frac{dv}{dt} = \frac{q}{m} \left(\frac{1}{2} r \times \frac{\partial B}{\partial t} + v \times B \right) \tag{2}$$

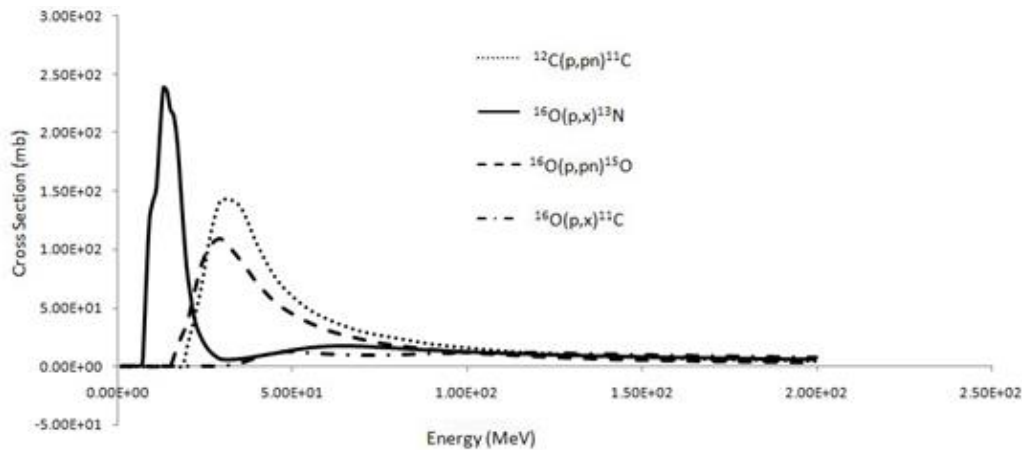


Figure 2. The cross-section versus the energy of the proton in the production of some positron emitters

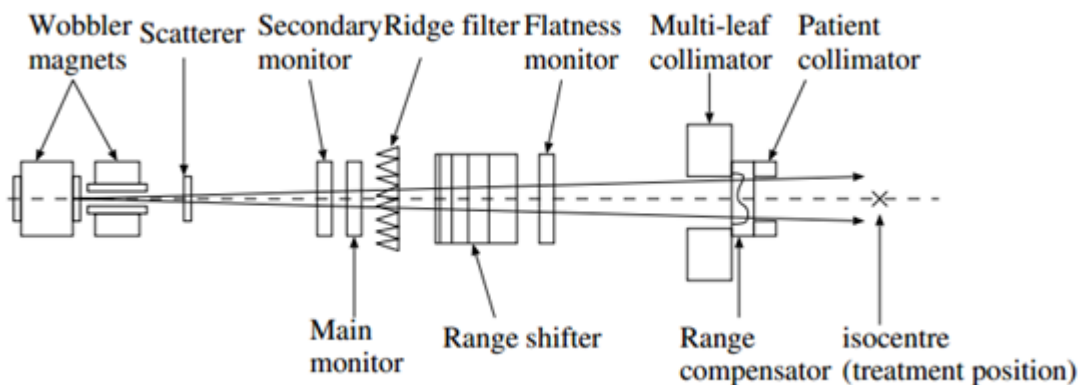


Figure 3. The proton therapy system in HIBMC

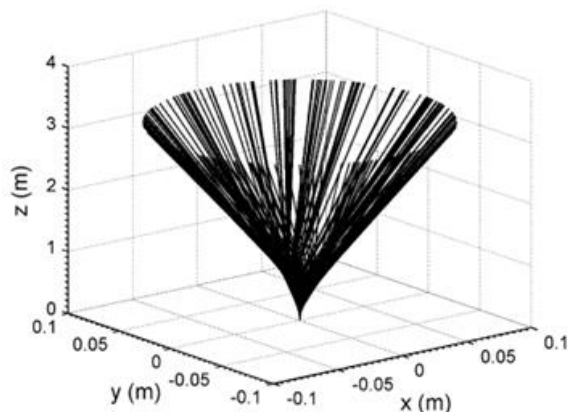


Figure 4. A beam of protons with an energy of 190 MeV after passing through 0.18 and 0.21 T fields in x and y directions, respectively

Protons have specific ranges in various materials; therefore, water was considered as the range shifter material to locate the Bragg peak exactly on the tumor. In order to localize the proton range exactly on the tumor, the range shifter thickness was determined 12 cm aligned with the beam direction.

The scatterer was considered as a copper metal sheet with a thickness of 0.245 cm according to Akagi et al. (12) in the simulation. The width of the Bragg peak should be 6cm for a tumor with a radius of 3 cm to receive a uniform dose value. To create a spread-out Bragg peak (SOBP) with 6 cm width, the protons should pass through a ridge filter with low atomic number materials which have various thicknesses using various steps. These thicknesses can be defined by the water equivalent depth. For instance, water equivalent depth of aluminium is 2.086 cm (14). In this simulation, the ridge filter was simulated based upon 6 steps. Therefore, the thickness of the steps was calculated to be 0.24, 0.48, 0.72, 0.96, 1.19, and 2.876 cm to have a SOBP thickness of 6 cm.

Before the beam collides to the target, the beam passes through an iron collimator, which has a hole with maximum dimensions of 16× 16 cm². Therefore, the results can be validated with those of Riazi et al. (13). When the head and the tumor are located in front of the device, the collimator's hole should be in accordance with the tumor size. Accordingly, when the head phantom is underexposed by the beam, the hole size of the collimator should be considered as a circular hole with r= 4cm (Figure 5).

At the first step, a cylindrical water phantom was used to design the ridge filter. Afterward, in order to measure the equivalent doses of the proton, neutron, and positron, a MIRD head phantom was used with a spherical tumor with the radius of r= 3 cm in its centre. The brain was defined using the following equations (15):

$$\left(\frac{x}{6.34}\right)^2 + \left(\frac{y}{8.26}\right)^2 + \left(\frac{z-51.5}{5.52}\right)^2 = 1 \tag{3}$$

$$\left(\frac{x}{6.9}\right)^2 + \left(\frac{y}{8.82}\right)^2 + \left(\frac{z-51.5}{6.08}\right)^2 = 1 \tag{4}$$

$$\left(\frac{x}{7.13}\right)^2 + \left(\frac{y}{9.05}\right)^2 + \left(\frac{z-51.5}{6.31}\right)^2 = 1 \tag{5}$$

$$\left(\frac{x}{7.22}\right)^2 + \left(\frac{y}{9.14}\right)^2 + \left(\frac{z-51.5}{6.4}\right)^2 = 1 \tag{6}$$

The equations 3-6 present brain, head, skull, and skin, respectively. The irradiated protons from the nozzle accelerator are in the Z direction.

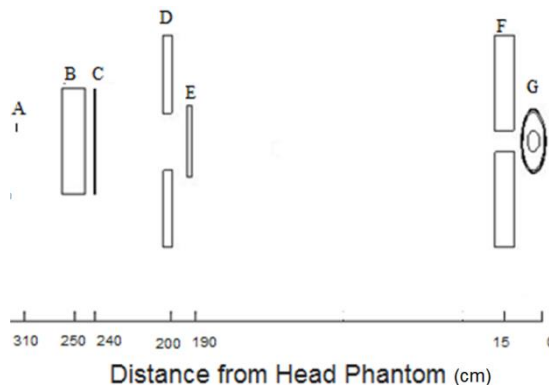


Figure 5. Proton therapy with simulated head phantom (MIRD), A denotes the source, B signifies range shifter, C indicates scatterer, D is the primary collimator, E represents ridge filter, F is collimator and G indicates the used phantom

Dosimetry by MCNPX Code

In this study, MCNPX2.6 was used with the LA 150 cross section library for protons and photons and 66 C for neutrons (16). However, F6 tally card is of no use to calculate secondary neutron dose. Therefore, to calculate secondary neutrons dose, the flux of neutron should be initially calculated by F4 tally. Subsequently, conversion factors should be applied using DF and DE cards. The DE and DF card values were obtained from the MCNPX user manual.

The equivalent dose regarding positrons and its annihilation photons can be calculated using the F6 tally card. It should be noticed that E card should be used to find the equivalent dose of photons with an energy of 0.511 MeV.

Results

Calculation of the Production Value of Positron-Emitting Nuclides by Monte Carlo Method

The dose and fluence of the proton were initially calculated to validate the results of this study. Figures 6 and 7 illustrate the results of this study, compared to those in a study conducted by Seravalli et al. (9). Moreover, the results show a relative difference within the range of about 1-3%, compared to the reference. As shown in Figure 6, protons have a sharp Bragg peak in the depth of 21.5 cm. In the primary area from zero to the depth of 18 cm, an almost fixed value of dose has arrived into the tissue. This value is equal to 30% of the maximum dose arrived in Bragg peak.

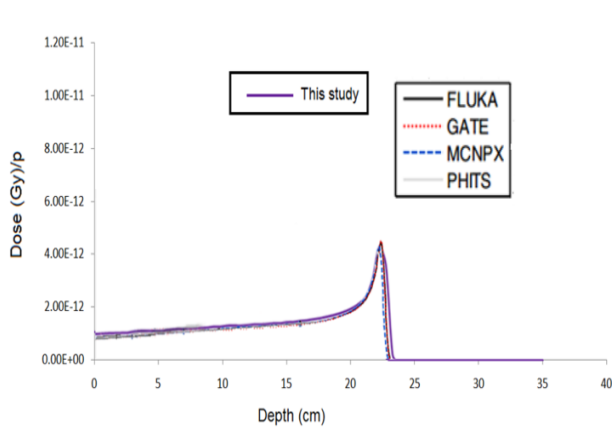


Figure 6. The absorbed dose of protons with the energy of 190 MeV in PMMA, the purple line showing the results of this study, whereas the other lines indicating the results of the study conducted by Seravalli et al. with FLUKA, Gate, MCNPX, and PHITS codes

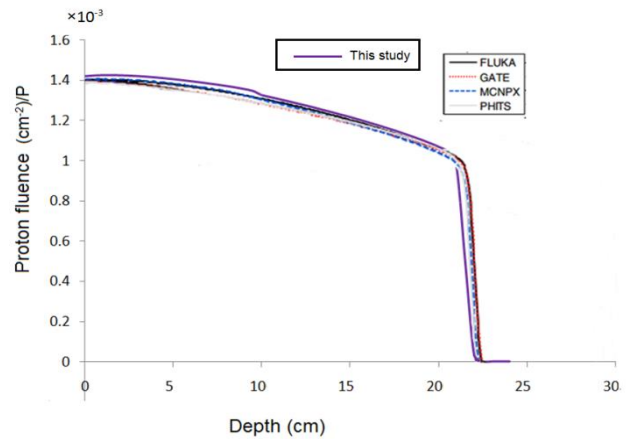


Figure 7. The fluence resulted from protons with the energy of 190 MeV in PMMA, the purple line showing the results of this study, whereas the other lines indicating the results of the study conducted by Seravalli et al. (9) with FLUKA, Gate, MCNPX, and PHITS codes

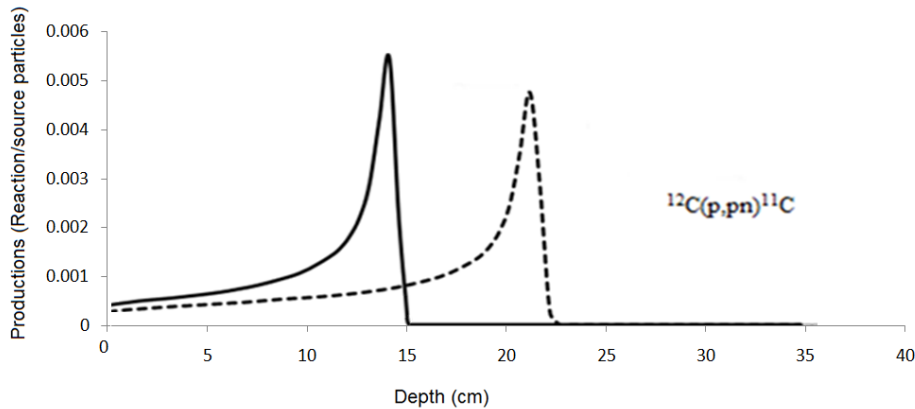


Figure 8. The production rate of ¹¹C versus depth resulted from the interaction of protons with the energy of 190 and 160 MeV

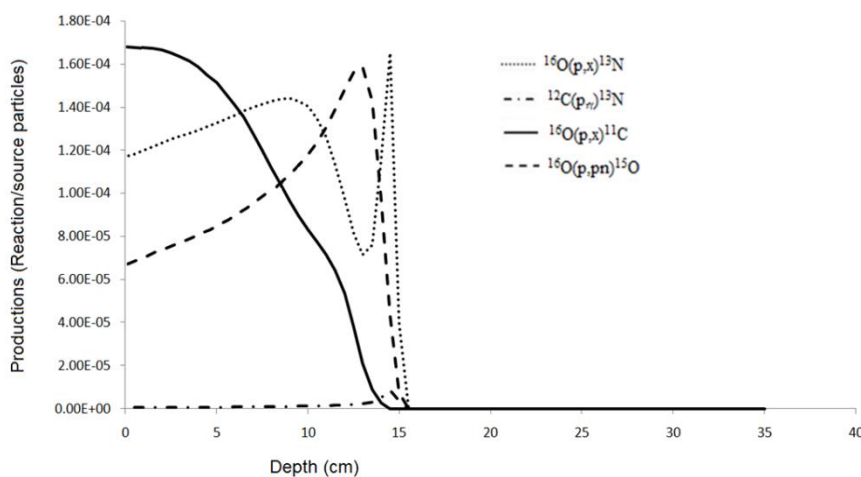


Figure 9. Production rate of ¹¹C ($T_{1/2}=20.6$ min) by ¹⁶O (p,x)¹¹C interaction and production rate of ¹³N ($T_{1/2}=9.96$ min) and ¹⁵O ($T_{1/2}=2.03$ min) by indicated interactions for protons energy of 160 MeV

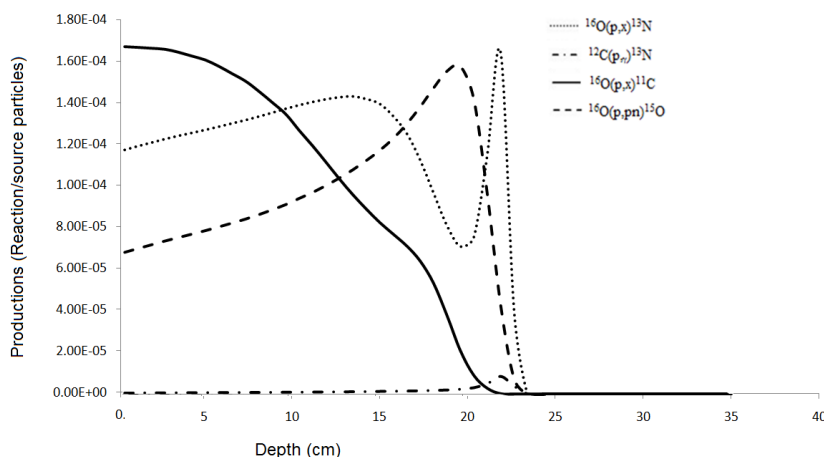


Figure 10. The production rate of ^{11}C ($T_{1/2}=20.6$ min) by ^{16}O (p,x) ^{11}C interaction and production rate of ^{13}N ($T_{1/2}=9.96$ min) and ^{15}O ($T_{1/2}=2.03$ min) by indicated interactions for proton energy of 190 MeV

Calculation of the Production Rate of Positron-Emitting Nuclides

As it is shown in Figure 8, the production rate of ^{11}C which is resulted from ^{12}C (p,x) ^{11}C interaction has a sharp peak in the Bragg peak area with a maximum of 4.4×10^{-3} and 4.1×10^{-3} for the proton energy beam of 160 and 190 MeV, respectively.

Figures 9 and 10 show the production rate of ^{11}C by ^{16}O (p,x) ^{11}C interaction and the production rate of ^{13}N and ^{15}O by proper interactions for proton energies of 190 and 160 MeV. From figures 8, 9 and 10, it can be concluded that the major production rate of ^{11}C belongs to ^{12}C (p,x) ^{11}C interaction.

The Results of Proton Therapy System Simulation for Water Phantom

A cylindrical water phantom was used and the relative dose of protons was calculated in proton energy of 190 MeV to make a comparison between the results of the current study and the reported results by Riazi et al. [13]. Figure 11 displays the obtained results and indicates that the SOBP in this study and the mentioned reference is 6 cm with a relative error of 3-8%.

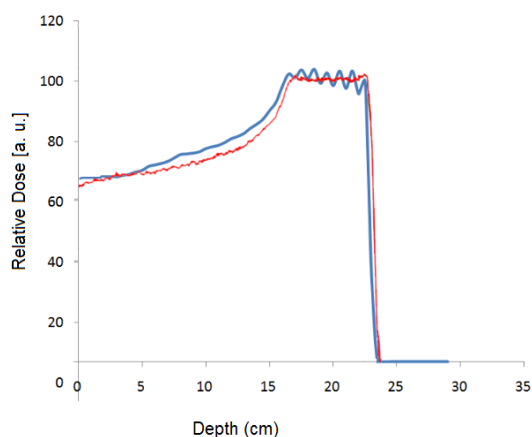


Figure 11. Comparison of the relative dose versus depth in this study (blue line) and reference (red line) in proton energy of 190 MeV

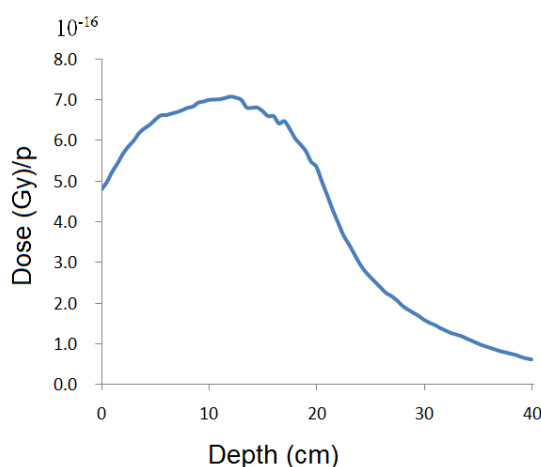


Figure 12. Dose versus depth for electrons when primary protons have the energy of 190 MeV

To have a sense about the dose distribution of secondary particles, electron dose distribution is presented in Figure 12. As it is shown, due to the presence of electrons, the dose has a relatively broad peak and its highest dose deposit is in depth of 12 cm and it never falls to zero in the phantom.

Calculation of Results of Equivalent Dose in MIRD Phantom

In this step, MIRD head phantom was exposed by the proton beam of proton therapy system as shown in Figure 5. Due to positron annihilation in various parts of the phantom, the equivalent dose of protons, neutrons, positrons, and photons was calculated regarding two energies of 190 and 160 MeV and has been tabulated in tables 2 and 3. All simulations were carried out using a core-i7 processor. The first simulation for 160 MeV protons and the second simulation for 190 MeV took 198.64 and 167.06 minutes with 10,000,000 histories, respectively.

Table 2. Equivalent dose of protons, neutrons, positrons, and photons in the head per one proton when input protons have the energy of 190 MeV

| Particle dose | Protons (Sv/P) | Neutrons (Sv/P) | Positrons (Sv/P) | Photons (Sv/P) | Total equivalent dose* (Sv/P) | Equivalent dose ratio** |
|---------------|----------------|-----------------|------------------|----------------|-------------------------------|-------------------------|
| Tumor | 3.96E-12 | 1.83E-14 | 3.99E-16 | 1.93E-18 | 3.98E-12 | 6.18E+01 |
| Brain | 6.60E-13 | 1.08E-14 | 1.77E-16 | 1.69E-18 | 6.71E-13 | 1.04E+01 |
| Skull | 3.80E-13 | 1.03E-14 | 1.59E-16 | 2.06E-18 | 3.90E-13 | 6.07E+00 |
| Skin | 1.39E-12 | 7.57E-15 | 1.32E-16 | 1.41E-18 | 1.40E-12 | 2.17E+01 |

* To calculate total equivalent dose and equivalent dose ratio, proton weighting factor was considered equal to 2 according to the ICRP103
 **Percentage of total equivalent dose in each tissue per total equivalent dose in the head

Table 3. Equivalent dose of protons, neutrons, positrons, and photons in the head per one proton when input protons have the energy of 160 MeV

| Particle dose | Protons (Sv/P) | Neutrons (Sv/P) | Positrons (Sv/P) | Photons (Sv/P) | Total equivalent dose* (Sv/P) | Equivalent dose ratio** |
|---------------|----------------|-----------------|------------------|----------------|-------------------------------|-------------------------|
| Tumor | 4.78E-12 | 7.61E-15 | 4.15E-16 | 1.89E-17 | 4.790E-12 | 6.24E+01 |
| Brain | 8.32E-13 | 4.94E-15 | 2.20E-16 | 1.48E-17 | 8.37E-13 | 1.09E+01 |
| Skull | 2.78E-13 | 4.71E-15 | 1.67E-16 | 1.54E-17 | 2.83E-13 | 3.69E+00 |
| Skin | 1.76E-12 | 3.45E-15 | 1.13E-16 | 1.89E-17 | 1.76E-12 | 2.30E+01 |

* To calculate total equivalent dose and equivalent dose ratio, proton weighting factor was considered equal to 2 according to the ICRP103
 **Percentage of total equivalent dose in each tissue per total equivalent dose in the head

As the tables show, the dose of the proton is maximum for both energy levels. For instance, proton dose for proton energy of 190 (160) MeV in the tumor is 6 (5.7) times more than proton dose in the healthy tissue of the brain. Moreover, it is 10 (17) and 2.8 (2.7) times more in the skull and skin, respectively.

As it is possible to predict from the figures 8, 9, and 10, the maximum value of positron emitting elements are produced in the Bragg peak area (tumor location). It must be noted that only some photons resulted from positron annihilation are absorbed inside the head. As shown in tables 2 and 3, there is a slight difference regarding the value of the equivalent dose of these photons in whole tissues of the head.

Discussion

To validate this study, dose and flux of protons were compared with those in a study conducted by Seravalli et al. (9) (figures 6 and 7). Seravalli et al. have simulated monoenergetic proton beam that was radiated to the simple cylindrical PMMA phantom by MCNPX, FLUKA, GATE, and PHITS. There is a 1-3% relative difference between the results of Seravalli et al. and the obtained results in this study. The production rates of ¹¹C, ¹³N, and ¹⁵O were calculated according to this system setup. As figures 8-10 show, ¹¹C has the most positron production rate, especially Bragg peak, compared to ¹³N and ¹⁵O.

In the next step, the results of the proton therapy nozzle simulation were compared with the published results by Riazi et al. (13). The simulation was done according to the proton therapy system in HIBMC for monoenergetic protons with an energy of 190 MeV. As can be seen in Figure 11, there was a 3-8% relative difference between the results of this study and those obtained from the study by Riazi et al. (13). It is mainly because of using different Monte Carlo codes. Riazi et al. used Geant 4 for the simulation of proton therapy

system while the MCNPX code was used for this purpose in this study.

To the best of our knowledge, this study was the first to calculate the production rate and adsorbed dose of positrons during proton-therapy of the brain. In addition, this study assessed the equivalent dose percentage in the healthy and tumoral tissue, compared to the total equivalent dose during brain proton therapy. According to the results of proton beam with the energy of 190 (160) MeV, the equivalent dose regarding the protons in the spherical tumor with the diameter of 6 cm, healthy tissue of brain, skull, and skin per proton particle were 3.98E-12 (4.79E-12), 6.71E-13 (8.37E-13), 3.90E-13 (2.83E-13), and 1.39E-12 (1.76E-12) (Sv/source particle), respectively. Furthermore, the ratio of equivalent dose using protons with the energy value of 190 (160) MeV in tumor, brain, skull, and skin to the total equivalent dose in the head regarding the primary and secondary particles were obtained at 61.8 (62.4) %, 10.4(10.9) %, 6.07(3.69) %, and 21.7(23) %, respectively.

Conclusion

In this study, the production rate of positron-emitting nuclides was initially calculated while a cylindrical PMMA phantom (r=35cm h=35cm) was under the bombardment of the proton beam with the energy of 190 MeV. The results demonstrated a considerable production value of positron-emitting nuclides including ¹¹C (T_{1/2}=20.3 min), ¹³N (T_{1/2}=9.96 min), and ¹⁵O (T_{1/2}=2.03 min). Meanwhile, the results showed that the production rate of ¹¹C was much more than the other abovementioned positron emitters. Therefore, the assessment of the production value of positron-emitting nuclides during proton therapy is very important in the dosimetry of tumor and healthy tissues. Therefore, the HIBMC proton therapy system and brain MIRD phantom were simulated by MCNPX 2.6 code to simulate the real conditions of brain proton therapy and calculate the equivalent dose in the tumor and healthy

tissues of the brain. According to the references, the most commonly used proton energies in brain tumor therapy are 160 and 190 MeV. As a result, these two energies were calculated along with the equivalent dose regarding protons and secondary particles, including neutron, positron, and gamma photons resulted from positron annihilation. A spherical tumor with a radius of 3 cm was located in the centre of brain MIRD phantom. Therefore, despite the fact that most of the equivalent dose is inside the tumor volume, the skin of the head has received a noticeable dose during proton therapy of brain which needs more concern.

Acknowledgment

The authors would like to thank Isfahan University of Technology for its financial support to conduct this research. The scientific collaboration of University of Isfahan is also appreciated.

References

1. Tavakol M, Karimian A, Aldaavati M. Dose Assessment of Eye and Its Components in Proton Therapy by Monte Carlo Method. *Iranian Journal of Medical Physics*. 2014;11(1):205-14.
2. Joshi B, Kushwaha M, Jain AK. On the discrepancy between proton and α -induced d-cluster knockout on 16O. *Progress of Theoretical and Experimental Physics*. 2016;2016(12).
3. Khan J, Kann BH, Pan W, Drachtman R, Roberts K, Parikh RR. Underutilization of proton therapy in the treatment of pediatric central nervous system tumors: an analysis of the National Cancer Database. *Acta Oncologica*. 2017;56(8):1122-5.
4. Farah J, Sayah R, Martinetti F, Donadille L, Lacoste V, Herault J, et al. Secondary neutron doses in proton therapy treatments of ocular melanoma and craniopharyngioma. *Radiation protection dosimetry*. 2014;161(1-4):363-7.
5. Zheng Y, Newhauser W, Fontenot J, Taddei P, Mohan R. Monte Carlo study of neutron dose equivalent during passive scattering proton therapy. *Physics in medicine and biology*. 2007; 52(15):4481-96.
6. Zheng Y, Liu Y, Zeidan O, Schreuder AN, Keole S. Measurements of neutron dose equivalent for a proton therapy center using uniform scanning proton beams. *Medical physics*. 2012; 39(6):3484-92.
7. Geng C, Moteabbed M, Seco J, Gao Y, Xu XG, Ramos-Méndez J, et al. Dose assessment for the fetus considering scattered and secondary radiation from photon and proton therapy when treating a brain tumor of the mother. *Physics in medicine and biology*. 2016; 61(2):683-95.
8. Kettern K, Coenen H, Qaim S. Quantification of radiation dose from short-lived positron emitters formed in human tissue under proton therapy conditions. *Radiation Physics and Chemistry*. 2009; 78(6):380-5.
9. Seravalli E, Robert C, Bauer J, Stichelbaut F, Kurz C, Smeets J, et al. Monte Carlo calculations of positron emitter yields in proton radiotherapy. *Physics in medicine and biology*. 2012;57(6):1659-73.
10. Reaction Rate. Available from: <https://www.nuclear-power.net/nuclear-power/reactor-physics/nuclear-engineering-fundamentals/neutron-nuclear-reactions/reaction-rate/>
11. TENDL-2014 Nuclear data library. Available from: http://ftp.nrg.eu/pub/www/talys/tendl2014/proton_html/proton.html.
12. Akagi T, Higashi A, Tsugami H, Sakamoto H, Masuda Y, Hishikawa Y. Ridge filter design for proton therapy at Hyogo Ion Beam Medical Center. *Physics in medicine and biology*. 2003; 48(22): 301-12.
13. Riazi Z, Afarideh H, Sadighi-Bonabi R. Fast numerical method for calculating the 3D proton dose profile in a single-ring wobbling spreading system. *Australasian Physical & Engineering Sciences in Medicine*. 2011; 34(3): 317-25.
14. Riazi Z, Afarideh H, Sadighi-Bonabi R. Influence of ridge filter material on the beam efficiency and secondary neutron production in a proton therapy system. *Zeitschrift für Medizinische Physik*. 2012; 22(3): 231-40.
15. Eckerman K. Description of the Mathematical Phantoms. 2002: 1-48.
16. ACE Libraries for Monte Carlo Transport Codes. <https://www-xdiv.lanl.gov/projects/data/nuclear/mcnpdata.html>.
17. ICRP, 2007. The 2007 Recommendations of the International Commission on Radiological Protection. ICRP Publication 103. *Ann. ICRP* 37 (2-4).